Journal of Alloys and Compounds 511 (2012) 70–73

Contents lists available at ScienceDirect

Journal of Alloys and Compounds

journal homepage: www.elsevier.com/locate/jallcom

Water-soluble Yb^{3+}, Tm^{3+} codoped $NaYF_4$ nanoparticles: Synthesis, characteristics and bioimaging

Huan Chen, Xuesong Zhai, Duo Li, Lili Wang, Dan Zhao*, Weiping Qin*

State Key Laboratory on Integrated Optoelectronics, College of Electronic Science & Engineering, Jilin University, Changchun 130012, China

ARTICLE INFO

Article history:
Received 15 March 2011
Received in revised form 8 August 2011
Accepted 9 August 2011
Available online 7 September 2011

Keywords:
$NaYF_4$
Upconversion
Water soluble
Nanoparticles

ABSTRACT

Water soluble $NaYF_4$ nanocrystals codoped with 20 mol% Yb^{3+}, 0.5 mol% Tm^{3+} were prepared by a facile solvothermal approach using polyvinylpyrrolidone (PVP) as a surfactant. The upconversion $NaYF_4$ nanocrystals were pure cubic phase with an average size of ~40 nm. They could be well redispersed in water to form a clearly transparent solution without obvious precipitation. With the excitation of a 980-nm diode laser, the nanocrystal solution presents bright violet and blue upconversion luminescence. These upconversion nanoparticles (UCNPs) were incubated with HeLa cells at 37 °C for 24 h, and bright blue upconversion luminescence were observed from the UCNPs endocytosed into the HeLa cells on a microscope equipped with a 980-nm fiber laser. These results indicated that the UCNPs had potential applications for biological imaging as luminescent probes.

1. Introduction

Upconversion (UC) is a nonlinear optical process that long-wavelength light can be converted to short-wavelength light by absorbing two or more pump photons [1]. UC materials have been widely used in many fields, including all-solid-state laser, full color display, optical communication, bio-labeling and so on [2,3]. Very recently, lanthanide (Ln)-doped UC nanoparticles (UCNPs) have attracted great attention as luminescent probes for bioimaging applications due to their remarkable advantages, such as large anti-Stokes shifts, narrow emission bandwidth, long fluorescence lifetime, and excellent photostability [4–7]. Compared with down-conversion probes, such as fluorescent organic dyes and quantum dots, the Ln-doped UC probes excited with near-infrared (NIR) light suffer much less the background autofluorescence that is usually encountered by ultraviolet (UV) pumping [8,9]. It also reaps the benefit of deep penetration into biological tissue by using a pumping light in the biological optical window of 800–1200 nm [10,11]. Furthermore, compared with high-energy UV excitation, low-energy NIR has the minimum photo-damage to the biological specimens [12].

$NaYF_4$ has been reported as the most efficient Ln-doped UC host material [13]. Under the 980 nm excitation, visible or UV emissions can be obtained via codoping Yb^{3+} ions as sensitizers, Tm^{3+} ions, Er^{3+} ions, or other rare earth (RE) ions as activators [14,15]. However, the RE ions codoped $NaYF_4$ materials should have the following properties in order to meet the demands as luminescent probes: (1) small size of sub-50 nm; (2) high dispersibility in water; (3) good biocompatibility; (4) strong UC luminescence in aqueous solutions [16,17]. It is worth noting that good water solubility and strong UC luminescence are especially the key factors. Li's group prepared oleic acid (OA)-capped UCNCs and used Lemieux-von Rudloff reagent to oxide the C=C double bond of OA and then obtained the water soluble nanocrystals [18]. Zhang's group synthesized silica-coated polyvinylpyrrolidone (PVP)/$NaYF_4$ nanocrystals which could dispersed in some of the most commonly used solvents, from weakly polar chloroform to strongly polar water [19]. However, it is still a challenge to synthesize UCNPs used as luminescent probes with good aqueous dispersibility and strong UC luminescence intensity.

In this paper, we report on water soluble, cubic phase $NaYF_4$: 20 mol% Yb^{3+}, 0.5 mol% Tm^{3+} UC nanocrystals prepared by a facile solvothermal method using PVP as the surfactant. These nanocrystals have an average size of ~40 nm with a narrow size distribution and can be well dispersed in water to form a clearly transparent solution. Under 980 nm excitation, the solution shows bright blue and violet emission that can be clearly seen with naked eye in day light. The HeLa cells could be labeled using these UCNPs as luminescent probes. These results indicated that the UCNPs had potential applications in biological field as luminescent probes.

2. Experimental

The initial chemicals, including Y_2O_3, Yb_2O_3, Tm_2O_3 (all with purity > 99.99%, Shanghai Shabo Chemical Technology Co., Ltd. China), hydrochloric acid (HCl,

* Corresponding authors. Tel.: +86 0431 85168241 8325;
fax: +86 0431 85168241 8325.
E-mail addresses: dzhao@jlu.edu.cn (D. Zhao), wpqin@jlu.edu.cn (W. Qin).

0925-8388/$ – see front matter © 2011 Elsevier B.V. All rights reserved.
doi:10.1016/j.jallcom.2011.08.043

37 wt%), ethylene glycol (EG, AR), polyvinylpyrrolidone K-30 (PVP, 58,000 g/mol) and sodium fluoride (NaF, AR), were used without further purification.

2.1. Synthesis of sample

Y_2O_3, Yb_2O_3, and Tm_2O_3 were dissolved in dilute hydrochloric acid to form $RECl_3$ (RE = Y, Yb, and Tm) solutions. After excess HCl and water were completely evaporated, the as-produced $RECl_3$ powders were dispersed in EG. 1 mmol $RECl_3$ (79.5 mol% YCl_3, 20 mol% $YbCl_3$, and 0.5 mol% $TmCl_3$) solutions were mixed together and 0.5 g PVP K-30 was added under stirring (the exact ratio of PVP to RE^{3+} is 1/116). This solution was labeled as solution A. 0.21 g NaF (the molecular ratio of F^- to RE^{3+} is 5/1) was dissolved in EG, then this NaF solution was added dropwise to the solution A. This mixture was kept stirring for at least 30 min, then it was transferred into a polytetrafluoroethylene autoclave and reacted at 150 °C for 24 h. After cooling to room temperature, the products was obtained by centrifugation and washed with deionized water and ethanol. To remove the residual NaF completely, the products should be washed with warm deionized water for several times. A part of precipitation was dried at 60 °C for 2 h and the other was redispersed in deionized water by ultrasonic treatment to get transparent solution.

2.2. Cell labeling with UCNPs

The HeLa cells were cultured (at 37 °C, 5% CO_2) on glass chamber slides in PRMI (Roswell Park Memorial Institute) 1640 medium containing 10% fetal bovine serum and 1% penicillin/streptomycin overnight in an incubator (Sanyo MCO-20AIC) for 24 h. The cells were gently washed three times with phosphate buffer solution (PBS). Then the HeLa cells were incubated with 300 μg/mL UCNPs for another 24 h in CO_2 incubator. After washing three times with PBS to remove excess UCNPs, the cells were imaged by an Olympus IX71 microscope equipped with a 980-nm fiber laser.

2.3. Measurements

The XRD analysis was carried out with a powder diffractometer (Model Rigaku RU-200b), using Ni-filtered Cu Kα radiation (λ = 1.5406 Å) with 200 mA current and 50 kV voltage across the tube to generate powerful X-ray. The XRD measurement was performed at a scan rate of 18° min^{-1} and step size of 0.02°. The morphology of the nanocrystals was investigated by FE-SEM (JEOL, JSM-6330F) and TEM (H-8100 200KV). A 2 W 980 nm continuous wave (CW) diode laser was used as the excitation source to study the UC luminescence of the sample. Their UC emission spectra were recorded with a fluorescence spectrometer (Hitachi F-4500). The UC luminescent pictures of the aqueous solution were taken by a Nikon digital camera (D300s). All the measurements were performed at room temperature.

3. Results and discussion

The XRD pattern of the $NaYF_4$: 20 mol% Yb^{3+}, 0.5 mol% Tm^{3+} sample is shown in Fig. 1, where the diffraction peaks are in good agreement with the data of cubic-phase $NaYF_4$ nanocrystals (JCPDS No. 6-342, α = 5.448 Å), and there no other peaks of impurities has been detected. It indicates that the products is single-phase pure cubic $NaYF_4$ crystals and demonstrates the highly crystalline nature of the nanocrystals. Although the as-prepared sample is cubic phase which has been reported to be less efficient than hexagonal-phase $NaYF_4$, the UCNPs we synthesized still has strong UC luminescence intensity. Fig. 2(a) and (b) shows the SEM and TEM images of the

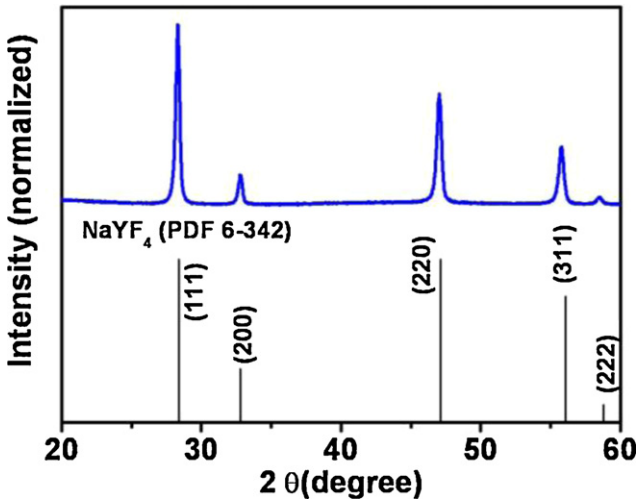

Fig. 1. (a) XRD pattern of the as-prepared UCNPs and standard data of cubic-phase $NaYF_4$ (JCPDS No. 6-342).

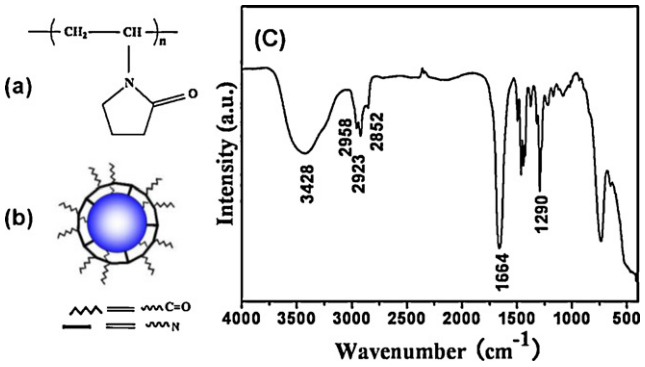

Fig. 3. (a) Molecular structure of PVP. (b) Scheme of the surface of PVP-modified UCNPs. (c) FTIR spectrum of the PVP-modified UCNPs.

cubic phase Yb^{3+}–Tm^{3+} codoped $NaYF_4$ nanocrystals. In the SEM image, we can see that the nanoparticles have small size contribution. In TEM image, it can be confirmed that the as-prepared UCNPs have an average size of ~40 nm. The small size of the nanoparticles sufficiently satisfies the demands of bio-applications as luminescent probes.

The molecular structure of PVP is given in Fig. 3(a). It is known that both the nitrogen and oxygen atoms have lone pair electrons which can combine with the empty orbital of metal ions. That

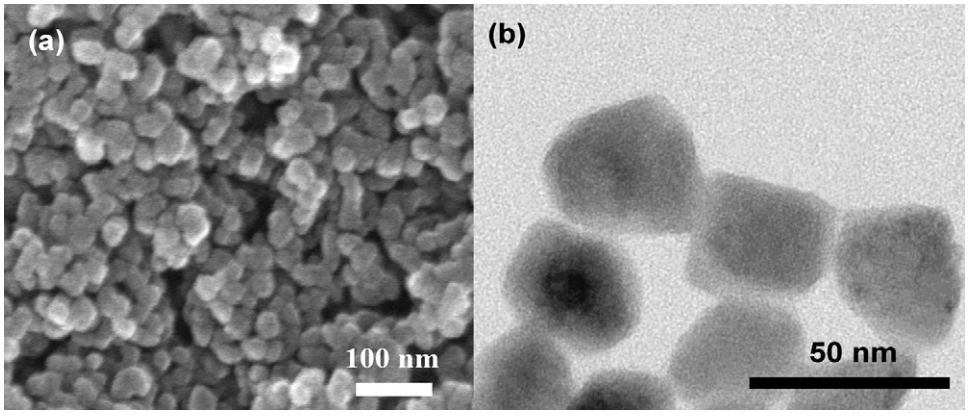

Fig. 2. (a) SEM and (b) TEM images of the UCNPs.

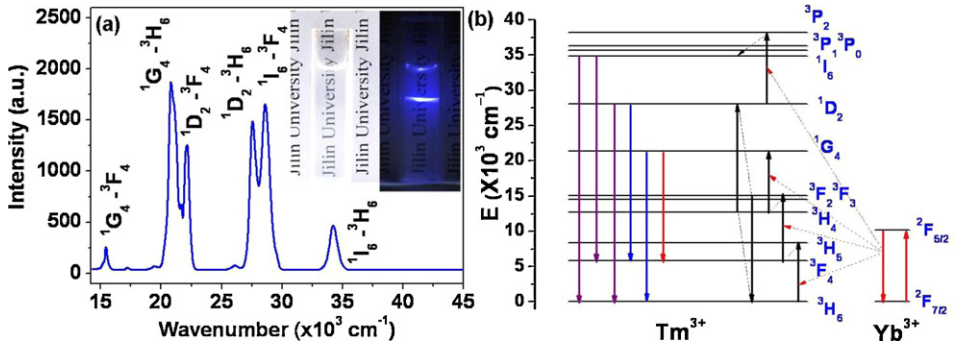

Fig. 4. (a) Upconversion spectrum of UCNPs under the excitation of 980 nm, insert: (left) photograph of the UCNPs dispersed in deionized water. (Right) Upconversion luminescence photograph of the same solution. (b) Energy level diagrams of Yb^{3+} ions and Tm^{3+} ions and the possible upconversion processes.

means the PVP molecules can well chelate with RE ions [20]. In the reaction process, the PVP acts as a chelating agent and could coordinate with RE ions. After the formation of UCNPs, it can act as an amphiphilic surfactant and drive the UCNPs dispersing in ethylene glycol or water. In our experiment, it can be supposed that the remains of PVP on the surface of UCNPs can form hydrogen bond with water molecules, as shown in Fig. 3(b). Presumably, this is why the UCNPs could be well dispersed in water and kept transparent for months. The photos of the UCNPs in water are shown in the insert of Fig. 4(a). The capping ligands on the surfaces of UCNPs were examined by Fourier transform infrared (FTIR) spectrum, as shown in Fig. 3(c). Some absorption bands in this spectrum confirm the presence of PVP molecules on the surfaces of UCNPs. The bands centered at 2958, 2923, and 2852 cm^{-1} are associated with the stretching vibration of methyl ($-CH_3$), the asymmetric (ν_{as}), and symmetric (ν_s) stretching vibrations of methylene ($-CH_2$), respectively. The band at 1290 cm^{-1} originates from the stretching vibration of carbon nitrogen bond (C–N) and the band at 1664 cm^{-1} originates from the vibration of carbon oxygen bond (C=O). The nitrogen and oxygen atoms can coordinate with the metal ions, leading to PVP molecules adhered to the surfaces of UCNPs. It should be noticed that the C=O groups (1664 cm^{-1}) on the surfaces of UCNPs can form hydrogen bonds with water molecules. The strong band around 3428 cm^{-1} can be attributed to the O–H stretching vibrations. Above analysis indicates that PVP molecules are well attached on the surface of the UCNPs, and therefore leading to the well dispersibility of nanocrystals in the solvents.

Both the as-prepared nanocrystals powders and their aqueous solution can emit visible and UV luminescence under the NIR excitation of 980 nm. We detect the UC spectrum using the 980 nm continuous wave diode laser as pumping source. The power of the focused laser is 140 mW. As shown in Fig. 4(a), there are characteristic peaks of Tm^{3+} ions in the UC spectrum of the aqueous solution. These peaks which center at 291, 350, 362, 450, 479, and 648 nm are attributed to the transitions of $^1I_6 \rightarrow {}^3H_6$, $^1I_6 \rightarrow {}^3F_4$, $^1D_2 \rightarrow {}^3H_6$, $^1D_2 \rightarrow {}^3F_4$, $^1G_4 \rightarrow {}^3H_6$, and $^1G_4 \rightarrow {}^3F_4$, respectively. The UC mechanism of NIR-to-visible/UV in this Yb^{3+}, Tm^{3+} codoped $NaYF_4$ system was studied [21]. Fig. 4(b) describes schematically possible upconverted processes in energy level diagrams of Yb^{3+} and Tm^{3+} ions. Under the excitation of 980 nm NIR, Yb^{3+} ions, served as sensitizers, absorb NIR photons and transfer the energy to Tm^{3+} ions to populate the excited states ($^3H_5$, $^3F_2$, and $^1G_4$) of Tm^{3+} ions. The cross-relaxation process of $^3F_{2,3} \rightarrow {}^3H_6$ (Tm^{3+}): $^3H_4 \rightarrow {}^1D_2$ (Tm^{3+}) may play the most important role in populating $^1D_2$. Thereafter, the state $^1I_6$ can be populated by the process of $^2F_{5/2} \rightarrow {}^2F_{7/2}$ (Yb^{3+}): $^1D_2 \rightarrow {}^1I_6$ (Tm^{3+}). In our experiments, the energy transfer from Yb^{3+} to Tm^{3+} is efficient, which resulted in effective population of Tm^{3+} ions in the high-energy state of $^1G_4$. From the spectrum in Fig. 4(a), we can see that the strongest peak is centered at 479 nm, and therefore the UCNPs dispersed aqueous solution exhibits bright blue luminescence under the excitation of 980 nm NIR, as shown in the insert of Fig. 4(a). The excellent transparency also can be seen from these photos. Through the solution the background words can be well distinguished.

For further investigation of their applicability as luminescent probes, the UCNPs were incubated with HeLa cells at 37 °C for 24 h. After washing with PBS to remove excess UCNPs, the living cells were imaged on an Olympus IX71 microscope equipped with a 980-nm NIR laser. Fig. 5(a) shows the bright-field images of the living HeLa cells that endocytosed UCNPs. We can observe that the cell morphology is good [22]. Then the sample was excited in situ by the 980-nm laser. We can clearly see the bright upconversion luminescence in the image of Fig. 5(b). (For interpretation of the references to color in this figure, the reader is referred to the web version of the article.) The overlay images of the luminescence and the HeLa cells are shown in Fig. 5(c). We can see that the blue luminescence well overlaps the cells, which confirms that the UCNPs are successfully used as luminescent probes to label the cancer cells with strong UC luminescence. These results imply that the UCNPs are biocompatible and can be used as potential luminescent probes for biological imaging.

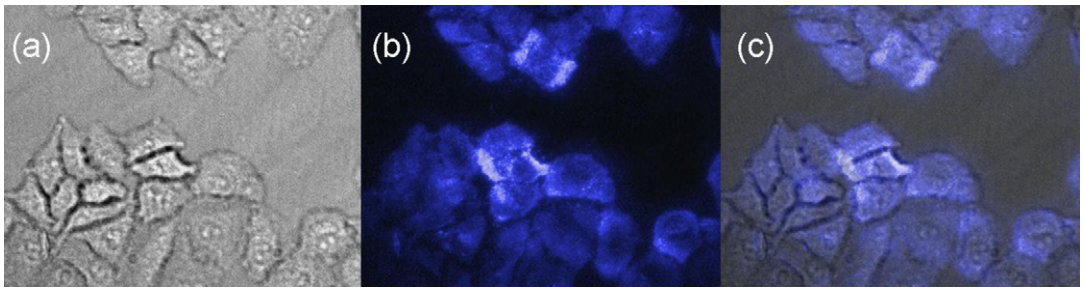

Fig. 5. (a) Bright-field image and (b) luminescence image under the excitation of 980 nm and (c) the overlay image of HeLa cells labeled with the UCNPs.

4. Conclusions

In conclusion, pure cubic-phase $NaYF_4$: 20 mol% Yb, 0.5 mol% Tm nanocrystals were prepared using PVP as the surfactant. The UCNPs can be well dispersed in water and the solution could be kept for months without obvious precipitation. Under NIR excitation of 980 nm, the solution presented bright violet/blue UC luminescence. Furthermore, the image of the UCNPs labeled cancer cells under 980-nm excitation confirmed that the UCNPs were biocompatible and could be use as luminescent probes. The as-prepared UCNPs have potential applications in biological field.

Acknowledgments

This work was supported by the National High Technology Research and Development Program of China (863 Program: 2009AA03Z309) and the National Natural Science Foundation of China (NNSFC) (grants 60908031 and 51072065).

References

[1] F. Auzel, Chem. Rev. 104 (2004) 139–174.
[2] T. Sandrock, H. Scheife, E. Heumann, G. Huber, Opt. Lett. 22 (1997) 808–810.
[3] E. Downing, L. Hesselink, J. Ralston, R. Macfarlane, Science 273 (1996) 1185–1189.
[4] S.V. Eliseevaa, J.C. Bünzli, Chem. Soc. Rev. 39 (2010) 189–227.
[5] K.Z. Zheng, D. Zhao, D.S. Zhang, N. Liu, F. Shi, W.P. Qin, J. Alloys Compd. 509 (2011) 5848–5852.
[6] S. Heer, K. Kömpe, H.U. Güdel, M. Haase, Adv. Mater. 16 (2004) 23–24.
[7] J.C. Boyer, F. Vetrone, L.A. Cuccia, J.A. Capobianco, J. Am. Chem. Soc. 128 (2006) 7444–7445.
[8] F. Wang, X.G. Liu, Chem. Soc. Rev. 38 (2009) 976–989.
[9] M. Wang, C.C. Mi, J.L. Liu, X.L. Wu, Y.X. Zhang, W. Hou, F. Li, S.K. Xu, J. Alloys Compd. 485 (2009) L24–L27.
[10] G.S. Yi, G.M. Chow, Adv. Funct. Mater. 16 (2006) 2324–2329.
[11] D.K. Chatterjee, A.J. Rufailah, Y. Zhang, Biomaterials 29 (2008) 937–943.
[12] Y.L. Song, Q.W. Tian, R.J. Zou, Z.G. Chen, J.M. Yang, J.Q. Hu, J. Alloys Compd. 509 (2011) 6539–6544.
[13] G.F. Wang, W.P. Qin, J.S. Zhang, L.L. Wang, G.D. Wei, P.F. Zhu, R.J. Kim, J. Alloys Compd. 475 (2009) 452–455.
[14] L.L. Wang, X.J. Xue, F. Shi, D. Zhao, D.S. Zhang, K.Z. Zheng, G.F. Wang, C.F. He, R.J. Kim, W.P. Qin, Opt. Lett. 34 (2009) 2781–2783.
[15] I.I. Leonidov, V.G. Zubkov, A.P. Tyutyunnik, N.V. Tarakina, L.L. Surat, O.V. Koryakova, E.G. Vovkotrub, J. Alloys Compd. 509 (2011) 1339–1346.
[16] W.C.W. Chan, S. Nie, Science 281 (1998) 2016–2018.
[17] G.S. Yi, G.M. Chow, Chem. Mater. 19 (2007) 341–343.
[18] Z.G. Chen, H.L. Chen, H. Hu, M.X. Yu, F.Y. Li, Q. Zhang, Z.G. Zhou, T. Yi, C.H. Huang, J. Am. Chem. Soc. 130 (2008) 3023–3029.
[19] Z.Q. Li, Y. Zhang, Angew. Chem. Int. Ed. 45 (2006) 7732–7735.
[20] H.S. Wang, X.L. Qiao, J.G. Chen, X.J. Wang, S.Y. Ding, Mater. Chem. Phys. 94 (2005) 449–453.
[21] K.Z. Zheng, L.L. Wang, D.S. Zhang, D. Zhao, W.P. Qin, Opt. Express 18 (2010) 2934–2939.
[22] E. Boatman, F. Cartwright, G. Kenny, Cell Tissue Res. 170 (1976) 1–16.